CHEMISTRY OF MATERIALS

Article

pubs.acs.org/cm

Hydroxyhexafluoroisopropylnorbornene Block and Random Copolymers via Vinyl Addition Polymerization and Their Application as Biobutanol Pervaporation Membranes

Dong-Gyun Kim,[†] Tamami Takigawa,[‡] Tomomasa Kashino,[‡] Oleksandr Burtovyy,[‡] Andrew Bell,[‡] and Richard A. Register*[,†]

[†]Department of Chemical and Biological Engineering, Princeton University, Princeton, New Jersey 08544, United States

[‡]Promerus, LLC, 9921 Brecksville Road, Brecksville, Ohio 44141, United States

Supporting Information

ABSTRACT: Vinyl addition polymers of substituted norbornene (NB) monomers possess very high glass-transition temperatures, making them useful in diverse applications; however, until very recently, the lack of an applicable living polymerization chemistry has precluded the synthesis of such polymers with controlled architecture, or copolymers with controlled sequence distribution. In the present work, block and random copolymers of NB monomers bearing hydroxyhexafluoroisopropyl and *n*-butyl substituents (HFANB and BuNB) are synthesized via living vinyl addition polymerization, using (η^3-allyl)Pd(*i*-Pr$_3$P)Cl activated by [Li(OEt$_2$)$_{2.5}$]B(C$_6$F$_5$)$_4$ as the initiator. Both series of polymers are cast into the selective skin layers of thin film composite (TFC) membranes, and these organophilic membranes are investigated for the concentration of *n*-butanol from dilute aqueous solution via pervaporation. The block copolymers show well-defined microphase-separated morphologies, both in bulk and as the selective skin layers on TFC membranes, while the random copolymers are homogeneous. Both block and random vinyl addition copolymers are effective as *n*-butanol pervaporation membranes, with the block copolymers showing a better flux-selectivity balance; the optimal block copolymer, containing 19 wt % BuNB, showed a process separation factor of 21 and a flux of 4300 g m^{-2} h^{-1} with a 1.00 wt % aqueous *n*-butanol feed, at a selective layer thickness of 1.3 μm. While polyHFANB has much higher permeability and selectivity than polyBuNB, incorporating BuNB units into the polymer (in either a block or random sequence) limits the swelling of the polyHFANB and thereby improves the *n*-butanol pervaporation selectivity. An analogous block copolymer derived from ring-opening metathesis polymerization, which shows much greater swelling than the vinyl addition polymers, shows a correspondingly higher flux and lower selectivity.

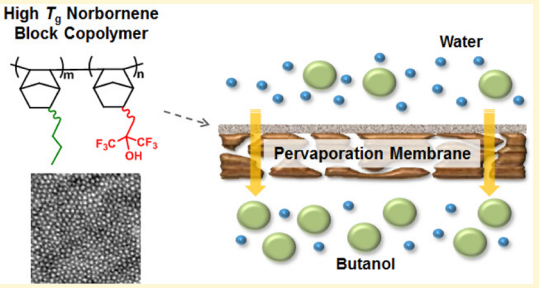

INTRODUCTION

Polynorbornene (polyNB), enchained via vinyl addition polymerization, has received considerable attention, because of its high glass-transition temperature ($T_g \approx 385$ °C[1]), good thermal stability, and low dielectric constant, compared with polyNBs prepared by ring-opening metathesis polymerization (ROMP) and cationic or radical polymerization.[2] These properties originate from the saturated bicyclic backbone structure of vinyl addition polyNB.[2] Although vinyl addition polyNB is poorly soluble in common organic solvents, which hampers its processing, vinyl addition polymers from substituted NB monomers possess much improved polymer solubility while still preserving the high T_g and good thermal stability of polyNB.[1,3−8] Based on these properties, vinyl addition polymers from substituted NBs are employed in microelectronics applications, including as dielectric materials,[1,3] photoresists,[4,5] and electro-optical materials.[6] Vinyl addition polyNBs with trimethylsilyl and sulfonic acid substituents have also been investigated as gas separation[7] and proton-conducting membranes,[8] demonstrating the excellent mechanical and film-forming properties of these polymers.

Renewable biofuels, such as ethanol[9] and butanol[10] synthesized via fermentation, are of increasing interest as alternatives to fossil fuels. Biobutanol (either *n*-butanol or isobutanol) has several advantages over bioethanol, including higher energy density, lower volatility/flammability, lower corrosiveness, lower hydrophilicity, and compatibility with existing gasoline supply infrastructure.[10] However, biobutanol production is limited by the low final concentration of butanol (~13 g L^{-1} *n*-BuOH in the traditional acetone−butanol−ethanol (ABE) fermentation process), leading to a high separations cost when the butanol is recovered by distillation.[11,12] Pervaporation,[13] wherein the butanol is recovered by selective transport through a membrane separating the liquid fermentation broth from a downstream vapor permeate, is thus

Received: August 6, 2015
Revised: September 3, 2015
Published: September 4, 2015

DOI: 10.1021/acs.chemmater.5b03030
Chem. Mater. 2015, 27, 6791−6801

Scheme 1. Synthesis of (a) Block and (b) Random Copolymers of HFANB and BuNB via Living Vinyl Addition Polymerization[a]

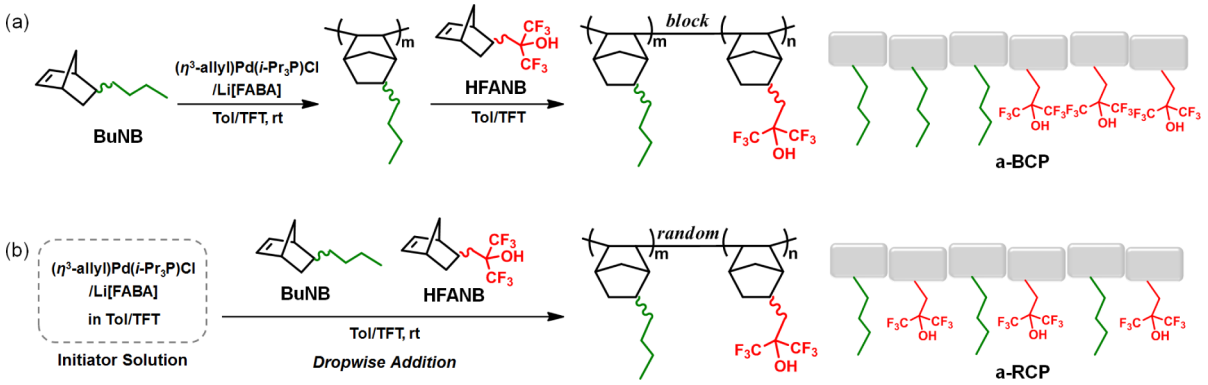

[a]Tol = toluene, TFT = α,α,α-trifluorotoluene.

of great interest, because of its potential for energy efficiency and compatibility with the broth's microorganisms.[12] Poly(dimethylsiloxane),[14−21] poly(ether-*block*-amide),[22] and poly[1-(trimethylsilyl)-1-propyne][15,23] membranes have been investigated for biobutanol recovery via pervaporation; since the separation in these membranes is based on the usual solution-diffusion mechanism,[13,24] it is essential that the solubility of butanol in the membrane be much higher than the solubility of water (i.e., that the membranes be organophilic/hydrophobic), to more than compensate for the larger molecular size and anticipated slower diffusion of butanol versus water. Vinyl addition polymers of substituted NBs possess not only the excellent mechanical and film-forming properties required for a membrane, but also a hydrophobic backbone structure coupled with a variety of available substituent groups, which can be selected to favor the solubility of organic permeants (such as butanol) within the membrane, making them attractive candidates for pervaporation applications.[25]

While the enchainment of substituted NB monomers into polymers of well-controlled architecture (including block copolymers) by "living" ROMP is now well-established,[26] comparable control over vinyl addition polymerizations of these same monomers has been elusive until recently, when a *t*-Bu_3P-ligated methylpalladium complex[27] was shown to initiate the living polymerization of NB monomers bearing a range of substituents, including hydroxyhexafluoroisopropyl (HFA).[28] PolyHFANB has been previously investigated as a lithographic photoresist;[5] it is soluble in butanol,[29] and shows particular promise as a butanol-selective component in pervaporation membranes.[25] Incorporating butanol-insoluble units, such as alkylnorbornene monomers (e.g., *n*-butylnorbornene, BuNB), into the polymer should permit some control over the extent of swelling of the membranes in aqueous butanol solutions. Unfortunately, polymerizations of HFA-substituted NB with the *t*-Bu_3P-ligated methylpalladium complex are relatively slow, and do not proceed to completion even within 2 days.[28] Faster polymerizations would allow for not only the synthesis of well-defined block copolymers, where the composition is controlled simply by the ratio of monomer charges, but also narrow-distribution, gradient-free random copolymers, synthesized by controlled (slow) addition of the monomer mixture to the reaction medium, as illustrated in Scheme 1.

In the present work, we employ a related initiator, (η^3-allyl)Pd(*i*-Pr_3P)Cl activated by $[Li(OEt_2)_{2.5}]B(C_6F_5)_4$, wherein the bulky *t*-$Bu_3$ phosphine ligands[28] are replaced by *i*-Pr_3 ligands to achieve much more rapid polymerizations, and thereby synthesize well-defined block and random copolymers of HFANB and BuNB. Recently, Ye et al.[29] studied the mechanical properties of a particular polyHFANB-*b*-polyBuNB (60 wt % HFANB), synthesized according to Scheme 1a, before and after solvent vapor annealing and immersion in an aqueous *n*-BuOH solution. Herein, we describe the synthetic route and demonstrate its applicability to synthesize block copolymers of targeted composition and molecular weight, as well as gradient-free random copolymers; we also fabricate thin film composite (TFC) membranes from these block and random copolymers, and from an analogous ROMP-derived block copolymer, and test their performance in *n*-BuOH recovery, revealing how their pervaporation performance is influenced by macromolecular composition and architecture.

EXPERIMENTAL SECTION

Materials. BuNB (5-butylnorbornene, 77/23 *endo*/*exo* ratio) was prepared via high-temperature Diels−Alder reaction of cyclopentadiene (CPD, charged as the dimer, dicyclopentadiene, DCPD) with 1-hexene.[30,31] HFANB (2-(bicyclo[2.2.1]hept-5-en-2-ylmethyl)-1,1,1,3,3,3-hexafluoropropan-2-ol, 82/18 *endo*/*exo*, >99.5%) was purchased from Central Glass Co., Ltd. (Japan). The monomers were stored under nitrogen atmosphere. Prior to polymerization, each monomer was degassed by freeze−pump−thaw cycles and stored over 3 Å molecular sieves in a nitrogen-filled MBraun Unilab glovebox (<0.1 ppm of O_2 and H_2O). Lithium tetrakis(pentafluorophenyl)-borate·($2.5Et_2O$) (Li[FABA]) was obtained from Boulder Scientific Co. and used as received. (Allyl)palladium(triisopropylphosphine) chloride ((η^3-allyl)Pd(*i*-Pr_3P)Cl) was synthesized as described previously.[32] The first-generation Grubbs initiator bis-(tricyclohexylphosphine)benzylidene ruthenium(IV) dichloride (97%), tricyclohexylphosphine (PCy_3), ethyl vinyl ether (99%), α,α,α-trifluorotoluene (TFT, anhydrous, ≥ 99%, Sure/Seal), *n*-butanol (*n*-BuOH, ≥ 99.7%), and anisole (anhydrous, 99.7%, Sure/Seal) were purchased from Sigma−Aldrich and used as received. Pd(0) hydrogenation catalyst supported on $CaCO_3$ (5 wt % Pd) was used as received from Alfa Aesar. Toluene was purified by passing through a solvent purification system (MBraun) integrated into the glovebox employed for polymerizations. All other reagents and solvents were used as received from standard vendors.

Synthesis of Homopolymers via Vinyl Addition Polymerization. Vinyl addition polymerization of BuNB or HFANB was conducted at room temperature under a nitrogen atmosphere in an MBraun Unilab glovebox (<0.1 ppm of O_2 and H_2O). The initial monomer concentration was 5 wt %. Aliquots were taken and quenched with acetonitrile at various times to monitor monomer conversion and molecular weight, each as a function of time. Anisole

DOI: 10.1021/acs.chemmater.5b03030
Chem. Mater. 2015, 27, 6791−6801

was included in the polymerization (1 equiv anisole per 4 equiv monomer) to permit the determination of monomer conversion from the aliquots using ^{1}H NMR spectroscopy, via the areas of the anisole methoxy protons and monomer olefin protons. The following procedure was used for the preparation of polyHFANB (entry 5 in Table 1, presented later in this work): HFANB (4.1 g, 0.015 mol) and toluene/TFT (78 g, 50/50 wt %) were placed into a 250 mL round-bottomed flask equipped with a magnetic stirring bar, and the mixture was stirred for 5 min before the injection of initiator solution. To a vial with a magnetic stirring bar, 0.15 mL of 0.50 M solution of (η^3-allyl)Pd(*i*-Pr$_3$P)Cl in TFT (26 mg, 0.075 mmol) and 0.15 mL of 0.50 M solution of Li[FABA] in TFT (65 mg, 0.075 mmol) were added and stirred for 20 min to activate the Pd pro-initiator. 0.20 mL of the (η^3-allyl)Pd(*i*-Pr$_3$P)Cl/Li[FABA] solution (0.050 mmol each of (η^3-allyl)Pd(*i*-Pr$_3$P)Cl and Li[FABA]) was injected into the flask containing the HFANB solution at once under vigorous stirring. After polymerization, the solution was precipitated into an excess of methanol (MeOH)/H_2O (50/50 vol %). The polymer so obtained was dissolved in tetrahydrofuran (THF), and the solution was stirred over activated charcoal, followed by passing through an alumina plug to remove Pd residue. The resulting filtrate was precipitated into MeOH/H_2O (50/50 vol %), and subsequently dried under vacuum at 60 °C. Homopolymers of different molecular weights were prepared using the same procedure, varying the monomer-to-initiator feed ratio ($[M]_0/[Pd]$; see Table 1, presented later in this work).

Synthesis of PolyHFANB-*b*-PolyBuNB via Vinyl Addition Polymerization. Vinyl addition block copolymers of HFANB and BuNB were synthesized and recovered similarly to the homopolymers, but employing sequential additions of the two monomers (Scheme 1a). The block copolymers are designated hereafter as a-BCP#, where "a" indicates "vinyl addition polymer", "BCP" indicates "block copolymer", and "#" indicates the weight percentage of HFANB in the polymer. The initial BuNB monomer concentration was 5 wt %, and the subsequent HFANB monomer charge was made as a 5 wt % solution. The following procedure was used for the preparation of a-BCP81 in Table 2 (presented later in this work): BuNB (0.99 g, 6.6 mmol) and toluene/TFT (19 g, 50/50 wt %) were placed into a 250 mL round-bottomed flask with a magnetic stirring bar, and 0.30 mL of (η^3-allyl)Pd(*i*-Pr$_3$P)Cl/Li[FABA] solution (0.075 mmol each of (η^3-allyl)Pd(*i*-Pr$_3$P)Cl and Li[FABA]) was injected into the flask at once, under vigorous stirring. After the complete consumption of BuNB (15 min), a small aliquot of the reaction mixture was taken and quenched with acetonitrile for GPC analysis of the polyBuNB block. HFANB (4.4 g, 16 mmol) in toluene/TFT (83 g, 50/50 wt %) was then added to the reaction flask and allowed to polymerize for 3 h. a-BCPs of different compositions were prepared using the same procedure, varying the ratio of the BuNB and HFANB monomer charges (Table 2, presented later in this work).

Synthesis of Poly(HFANB-*r*-BuNB) via Vinyl Addition Polymerization. Vinyl addition random copolymers of HFANB and BuNB were synthesized and recovered similarly, but employing slow (dropwise) addition of the monomer mixture (Scheme 1b). The random copolymers are designated as a-RCP#, where "a" indicates "vinyl addition polymer", "RCP" indicates "random copolymer", and "#" indicates the wt % of HFANB in the polymer. The following procedure was used for the preparation of a-RCP64 in Table 2 (presented later in this work): 0.24 mL of (η^3-allyl)Pd(*i*-Pr$_3$P)Cl/Li[FABA] solution (0.059 mmol each of (η^3-allyl)Pd(*i*-Pr$_3$P)Cl and Li[FABA]) was injected into a 250 mL round-bottomed flask containing toluene/TFT (21 g, 50/50 wt %) and a magnetic stirring bar. A mixture of HFANB (2.4 g, 8.8 mmol), BuNB (1.3 g, 8.8 mmol), and toluene/TFT (49 g, 50/50 wt %) was placed into a dropping funnel mounted on the round-bottomed flask, and the monomer solution was added dropwise to the reaction mixture (15 s per drop) under vigorous stirring; the complete addition of monomer solution took more than 10 h. Other a-RCPs were prepared using the same procedure, varying the composition of the monomer mixture charged to the addition funnel (Table 2, presented later in this work).

Synthesis of PolyHFANB-*b*-PolyBuNB via ROMP, and Subsequent Hydrogenation. A ROMP block copolymer of HFANB and Bul;NB (r-BCP81; see Scheme S1 in the Supporting Information and Table 1 (presented later in this work)) was synthesized by sequential addition of the monomers at room temperature under a nitrogen atmosphere in an MBraun Unilab glovebox (<0.1 ppm of O_2 and H_2O), followed by hydrogenation. The ROMP block copolymer is designated as r-BCP81, where "r" indicates "ROMP polymer", "BCP" indicates "block copolymer", and "81" indicates the 81 wt % HFANB content in the polymer. The initial BuNB monomer concentration was 4 wt % in toluene, and the subsequent HFANB monomer charge was made as a 4 wt % toluene solution. BuNB (0.8 g, 5.3 mmol) and toluene (19 g) were placed into a 250 mL round-bottomed flask equipped with a magnetic stirring bar, and the mixture was stirred for 5 min before the injection of initiator solution. To a vial with a magnetic stirring bar, bis-(tricyclohexylphosphine)benzylidene ruthenium(IV) dichloride (0.034 g, 0.05 mmol), PCy_3 (0.057 g, 0.20 mmol), and toluene (4 mL) were added and stirred for 5 min. The initiator solution was injected into the flask containing the BuNB solution at once under vigorous stirring. After the complete consumption of BuNB (1 h), a small aliquot of the reaction mixture was taken and terminated with an excess of ethyl vinyl ether for GPC analysis of the polyBuNB block. HFANB (3.4 g, 12 mmol) in toluene (81 g) was then added to the reaction flask. The HFANB was allowed to polymerize for 6 h. The block copolymer was terminated with an excess of ethyl vinyl ether and recovered by evaporating the solvent under N_2 flow. The polymer so obtained was dissolved in 1 L of cyclohexane/THF (95/5 vol %) and charged to a 2 L Parr reactor. Hydrogenation was conducted using Pd(0)/$CaCO_3$ (8.0 g) at 100 °C and 400−500 psig H_2 for 2 days. The progress of the reaction was tracked by ^{1}H NMR until olefinic double bonds were no longer detectable (>99.9% saturation). After removal of the Pd(0)/$CaCO_3$ by filtration, the resulting solution was concentrated, precipitated into MeOH/H_2O (50/50 vol %), and the polymer dried under vacuum at 60 °C.

Membrane Preparation. Thin film composite (TFC) membranes with dense polymer layers of an a-BCP, an a-RCP, or r-BCP81 as the thin selective skin layer were prepared via simple blade coating, using PAN-350 (Sepro Membranes) as the support; PAN-350 consists of a porous poly(acrylonitrile) (PAN) top layer on a poly(ethylene terephthalate) (PET) nonwoven backing. Each vinyl addition polymer was dissolved as a 10 wt % solution in a toluene/TFT/THF mixture (40/40/20 wt %) and filtered through a 0.45-μm-pore polytetrafluoroethylene filter. The polymer solution was poured onto a sheet of PAN-350 supported by a pane of glass, and the solution pulled across the membrane by a film casting knife (Tefcrom, Paul M. Gardner Company, Inc., 25 μm gap height) to form a film with uniform thickness. For the r-BCP81 membrane, a polymer concentration of 15 wt % and a 75 μm gap were employed to achieve a comparable selective layer thickness. The membranes were solvent-annealed at room temperature in a THF chamber (a glass tray, holding a layer of THF at the bottom and covered with aluminum foil; the TFC membrane, still on its glass pane, rests in the vessel's center, supported by pillars) for 2 h. The membrane was subsequently dried on a hot plate at 60 °C for 1 h, then under vacuum at 60 °C overnight, then peeled off the glass pane.

Pervaporation Measurements. Pervaporation was carried out on a home-built apparatus, as diagrammed in Scheme S2 in the Supporting Information. The effective area of the membrane was 13.38 cm^2. A 1.00 wt % *n*-BuOH aqueous solution was employed as the feed, circulated through the system at 450 mL min^{-1} by a diaphragm pump, and heated by passage through a heat exchanger (No. 00256-02, Exergy, LLC) connected to a heated water-bath circulator. After bypassing the membrane for 30 min to allow the feed to reach the desired temperature, the feed was directed into the crossflow membrane module (47 mm single stage filter assembly, Savillex Corp.) for 1 min to check for any leakage; once the absence of leaks was confirmed, vacuum was applied to the downstream side of the membrane (<10 Torr absolute pressure), and permeate was collected in a trap immersed in liquid nitrogen. The cold trap was weighed before and after the pervaporation experiment to calculate total mass flux (J). The composition of permeate was determined by

DOI: 10.1021/acs.chemmater.5b03030
Chem. Mater. 2015, 27, 6791−6801

^{1}H NMR using acetone-d_6 as a solvent; a small amount of anhydrous ethanol was added to the permeate to make the phases miscible, thus providing a single-phase solution which was sampled for NMR analysis. At least three different membranes were prepared from each polymer and tested in the pervaporation system. For the pervaporation stability test, two cold traps arranged in parallel were used to alternately collect permeate; at each switch between traps, makeup aqueous *n*-BuOH of the same composition as the permeate was added to the feed reservoir in an amount equal to the permeate collected, so that the *n*-BuOH feed concentration was kept at 1.00 wt % throughout the stability test. To eliminate the effect of variations in selective layer thickness (l) between membranes on the flux, a thickness-normalized flux (J', normalized to a membrane thickness of 2 μm) was employed:[24]

$$J = \frac{Q}{A \times t} \tag{1}$$

$$J' = J \times \left(\frac{l}{2}\right) \tag{2}$$

where Q is the total mass (in grams) of the permeate collected over time t (in hours), A is the effective area of the membrane (expressed in square meters), and l is the membrane thickness (polymer coating layer, given in micrometers). The process separation factor (β) was calculated as[33]

$$\beta = \frac{Y_{\mathrm{BuOH}}/(1 - Y_{\mathrm{BuOH}})}{X_{\mathrm{BuOH}}/(1 - X_{\mathrm{BuOH}})} \tag{3}$$

where X_{BuOH} and Y_{BuOH} represent the weight fractions of *n*-BuOH in the feed and permeate, respectively. The membrane permeabilities for water (P_w) and *n*-BuOH (P_b), along with the membrane selectivity α, were calculated as[33]

$$P_i = \frac{J_i l}{M_i x_i \gamma_i p_i^{\mathrm{sat}}} = \frac{J_i'(2\,\mu\mathrm{m})}{M_i x_i \gamma_i p_i^{\mathrm{sat}}} \tag{4}$$

$$\alpha = \beta\left(\frac{\gamma_w p_w^{\mathrm{sat}}}{\gamma_b p_b^{\mathrm{sat}}}\right) \tag{5}$$

where p_i^{sat} is the saturation vapor pressure of pure component i with molecular weight M_i, and γ_i is the liquid-phase activity coefficient of component i in the feed, at a mole fraction x_i. These expressions implicitly assume that the partial pressure of each component on the downstream side of the membrane is negligible, which is an appropriate assumption when the permeate is collected in a liquid-nitrogen-cooled trap.[33] In all cases, the selective layer thicknesses l employed for calculation were those measured on the dry membranes, neglecting any membrane swelling. Vapor pressures were calculated from published Antoine correlations[34] (at 60 °C, p_b^{sat} = 7.80 kPa, p_w^{sat} = 19.87 kPa; at 37 °C, p_b^{sat} = 1.98 kPa, p_w^{sat} = 6.26 kPa), while activity coefficients were calculated from a published NRTL (nonrandom two-liquid) correlation[34] based on data ("run 2") obtained at 50 °C (at 60 °C, γ_b = 66.0, γ_w = 1.00011; at 37 °C, γ_b = 102.6, γ_w = 1.00014; all at x_b = 0.002449 for 1.00 wt % *n*-BuOH). Note that the NRTL parameters[35] obtained by fitting to data[36] at 60 °C are quite similar (calculated activity coefficients at 37 and 60 °C differ by <0.6%).

Instrumentation and Characterization Techniques. ^{1}H NMR spectra of homopolymers were recorded on a Bruker AVANCE III 500 MHz spectrometer using $CDCl_3$ (for polyBuNB) or dimethyl sulfoxide-d_6 (for polyHFANB) as solvent. Monomer *endo*/*exo* ratios were also determined by ^{1}H NMR spectroscopy, on $CDCl_3$ solutions.[37] Copolymer compositions were determined by quantitative ^{13}C NMR spectroscopy in THF-d_8, using a Bruker AVANCE III 500 MHz spectrometer.[28] Polymer number-average molecular weights (M_n) and molecular weight dispersities ($Đ$) were determined by gel permeation chromatography (GPC) in THF, using a Waters 515 HPLC Pump, two 30 cm Agilent PLgel Mixed-C columns operating at 35 °C, and Wyatt OptiLab T-rEX (differential refractive index, RI) and miniDAWN TREOS (three-angle light scattering, LS) detectors, both operating at 658 nm and 25 °C. The GPC-RI elution time data were calibrated with narrow-distribution polystyrene standards. M_n values were taken from the light scattering data via the Wyatt Astra software (averaging over the elution time distribution), while the values of $Đ$ were taken from the GPC-RI data; $Đ$ as computed by the Astra software is generally much closer to unity (<1.05), for reasons previously discussed.[28] The specific refractive index increment (dn/dc, necessary for analysis of the light scattering data) for each vinyl addition homopolymer and r-BCP81 (after hydrogenation) in THF at 25 °C and 658 nm was determined using a separate Wyatt Optilab rEX; the values are 0.1321, 0.0437, and 0.0389 mL g^{-1} for polyBuNB, polyHFANB, and r-BCP81, respectively. The dn/dc values for the vinyl addition block and random copolymers were calculated as weight-fraction-weighted averages of the dn/dc values of the corresponding homopolymers,[38] using the weight fractions determined from ^{13}C NMR spectroscopy.

Differential scanning calorimetry (DSC) of polymers was run using a Perkin−Elmer DSC 7 system under a nitrogen atmosphere. Polymer samples with masses of 5−10 mg were encapsulated in sealed aluminum pans; they were first heated to 200 °C, then cooled to −50 °C at 10 °C min^{-1}, followed by a second heating scan from −50 °C to 200 °C at a heating rate of 10 °C min^{-1}.

Small-angle X-ray scattering (SAXS) patterns were acquired with an Anton-Paar compact Kratky camera equipped with an MBraun OED-50 M position-sensitive detector. Data were corrected for detector sensitivity and positional linearity, empty beam scattering, and sample thickness and transmittance, placed on an absolute intensity scale via a polyethylene standard, and desmeared for slit length.[39] Intensities are presented against the magnitude of the momentum transfer vector $q = (4\pi/\lambda)\sin\theta$, where θ is half the scattering angle. Silver behenate (d = 5.838 nm) was used to calibrate the scattering angle.[40] Free-standing polymer films (thickness ≈ 0.35 mm) were prepared by solution casting on a polytetrafluoroethylene sheet, using the same coating solution employed for the membrane preparation. The solvent was slowly evaporated in the THF chamber, followed by subsequent drying at 60 °C under vacuum.

The interaction of each polymer with dilute aqueous *n*-BuOH was characterized by two distinct methods. In the first method,[25] referenced below as "*n*-BuOH absorption", 0.20 g of finely ground polymer powder were added to 4.0 g of 1.00 wt % *n*-BuOH aqueous solution and stirred for 2 days. (For r-BCP81, which has a glass transition near room temperature and is thus difficult to grind into a free-flowing powder, small pieces of thin film were employed.) The concentration of *n*-BuOH in the supernatant was then analyzed by ^{1}H NMR, with the fractional decrease in *n*-BuOH concentration reflecting absorption by the polymer. In the second method, free-standing polymer films (thickness of ∼50 μm, prepared as done for SAXS, weighing 40−50 mg) were immersed into 20 g of 1.00 wt % *n*-BuOH (initial concentration) at room temperature for 2 days. The large excess of solution ensures that its *n*-BuOH concentration remains essentially constant (<5% depletion) as the film swells. Subsequently, the film was removed, blotted dry, and quickly weighed; the "degree of swelling" (DS) was calculated as

$$\mathrm{DS}\,(\%) = \frac{W_s - W_d}{W_d} \times 100 \tag{6}$$

where W_d and W_s are the weights of the dry and swollen polymer film, respectively.

Each membrane surface and cross-section was characterized by scanning electron microscopy (SEM) (FEI/Philips Model XL30 field-emission gun microscope). For cross-sectional imaging, the selective skin layer and the supporting PAN layer were peeled off together from the PET nonwoven backing using 3M tape. Then, the 3M tape/polymer/PAN sample was immersed into liquid nitrogen and fractured by bending to obtain a clean cross-section. The membrane surface morphology was characterized using atomic force microscopy (AFM) (Bruker Dimension 3000) in tapping mode (TM), using force modulation mode probes (force constant = 1.2−5.5 N m^{-1}, resonance

DOI: 10.1021/acs.chemmater.5b03030
Chem. Mater. 2015, 27, 6791−6801

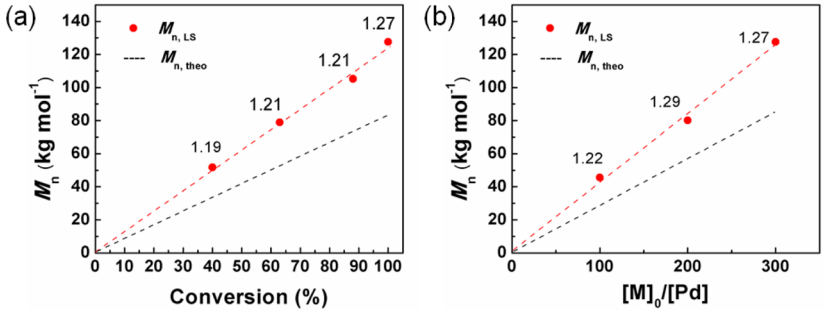

Figure 1. (a) M_n vs conversion ([M]$_0$/[Pd] = 300) and (b) M_n vs [M]$_0$/[Pd] (conversion =100%) for the vinyl addition polymerization of HFANB. The label next to each data point represents the molecular weight dispersity ($Đ$) of that polymer, as determined from GPC-RI.

Table 1. Living Vinyl Addition Polymerization of BuNB and HFANB Using (η^3-allyl)Pd(i-Pr$_3$P)Cl/Li[FABA][a]

entry	monomer[b] (*endo*/*exo*)	[M]$_0$/[Pd][c]	time (min)	conversion[d] (%)	$Đ$[e]	$M_{n, theo}$[f] (kg mol^{-1})	$M_{n, LS}$[g] (kg mol^{-1})
1	BuNB (77/23)	100	20	100	1.12	15.0	22.5
2	BuNB (77/23)	300	40	100	1.15	45.1	66.6
3	HFANB (82/18)	100	60	100	1.22	27.4	45.6
4	HFANB (82/18)	200	120	100	1.29	54.8	80.2
5	HFANB (82/18)	300	180	100	1.27	82.3	127.6

[a]5 wt % monomer in toluene/TFT (50/50 wt %), at room temperature. [b](*endo*/*exo*) is the ratio of *endo*- to *exo*-isomers in the monomer. [c](η^3-allyl)Pd(i-Pr$_3$P)Cl/Li[FABA] = 1/1. [d]Confirmed by ^{1}H NMR spectroscopy. [e]Determined by GPC in THF using a differential refractive index (RI) detector, calibrated with narrow-distribution polystyrene standards. [f]Theoretical molecular weight, calculated from [M]$_0$/[Pd] × $M_{monomer}$ × conversion/100%, where $M_{monomer}$ is the monomer molecular weight. [g]Determined by GPC using multiangle laser light scattering (LS).

Table 2. Characteristics of Block and Random Copolymers

polymer	W_{HFANB}[a]	DP[b] (polyHFANB−polyBuNB)	$M_{n, LS}$[b] (kg mol^{-1})	$Đ$[c]	solubility[d] in *n*-BuOH/H$_2$O	*n*-BuOH absorption[e] (%)	degree of swelling, DS (%)[f]
polyHFANB	1	465−0	128	1.27	S/I	52	16.1
a-BCP92	0.92	414−67	123	1.16	S/I	51	14.2
a-BCP81	0.81	300−130	102	1.12	S/I	48	12.4
a-BCP64	0.64	203−206	86	1.16	S/I	44	9.6
a-BCP37	0.37	106−332	79	1.13	I/I	36	6.0
a-RCP81	0.81	415[g]	98	1.40	S/I	50	14.4
a-RCP64	0.64	566[g]	120	1.29	S/I	47	10.7
a-RCP37	0.37	791[g]	143	2.65	I/I	37	6.1
polyBuNB	0	0−421	63	1.09	I/I	19	1.4
r-BCP81	0.81	298−128	101	1.24	S/I	30	31.8

[a]Weight fraction of HFANB in the polymer, determined by quantitative ^{13}C NMR spectroscopy (Figure S5); the values for the diblocks agree with those calculated from $M_{n, LS}$. [b]DP = degree of polymerization, as determined from $M_{n, LS}$. [c]Determined by GPC in THF using a differential refractive index (RI) detector, calibrated with narrow-distribution polystyrene standards. [d]S = soluble, I = insoluble. [e]Percentage of *n*-BuOH absorbed from an initially 1.00 wt % *n*-BuOH aqueous solution (4.0 g) by 0.2 g of polymer; average of three replicate measurements with a standard deviation of less than ±1%, except for r-BCP81 (±2.4%). [f]In 1.0 wt % *n*-BuOH, as defined in eq 6, average of three replicates with standard deviation ≤0.5% except for r-BCP81 (±0.8%). [g]Total DP.

frequency = 60−90 kHz) purchased from NanoWorld. All images were taken at 512 × 512 pixel resolution with a scan size of 2 μm × 2 μm.

RESULTS AND DISCUSSION

The (η^3-allyl)Pd(i-Pr$_3$P)Cl/Li[FABA] complex was indeed found to initiate rapid, living vinyl addition polymerization of BuNB and HFANB. For HFANB, Figure 1a shows that M_n increases linearly with conversion; at complete conversion, M_n also increases linearly with the monomer-to-initiator feed ratio ([M]$_0$/[Pd]), when the latter range was 100−300 (Figure 1b). Complete conversion of HFANB is achieved within 3 h, even at [M]$_0$/[Pd] = 300, and the molecular weight distributions remain monomodal and narrow ($Đ$ < 1.3; see Table 1) throughout (see Figures S1 and S2 in the Supporting Information). Polymerization of BuNB is even faster, reaching complete conversion within 40 min even at [M]$_0$/[Pd] = 300, and again showing a linear dependence of M_n on [M]$_0$/[Pd] (see data in Table 1) at complete conversion. PolyBuNB also generally shows a narrow and monomodal distribution, but at high monomer-to-initiator ratios ([M]$_0$/[Pd] = 300), once polymerization is essentially complete, additional peaks at higher molecular weight appear and grow, reflecting a branching side-reaction that proceeds slowly, relative to propagation (see Figure S3 in the Supporting Information). No olefinic proton peaks were observed in the ^{1}H NMR spectra of the BuNB and HFANB homopolymers (see Figure S4 in the Supporting Information), confirming that the polymerization mechanism is exclusively vinyl addition polymerization, not ROMP. From the ratio of $M_{n, theo}$/$M_{n, LS}$ (values given in Table 1), the efficiency of the initiator complex is consistently 64% ± 4%, which allows for the synthesis of polymers of precisely targeted M_n.

DOI: 10.1021/acs.chemmater.5b03030
Chem. Mater. 2015, 27, 6791−6801

A series of well-defined HFANB-BuNB vinyl addition diblock copolymers (a-BCP#, where # is the weight percentage of HFANB in the diblock) with different compositions were synthesized by sequential monomer addition (Scheme 1a), BuNB block first, with a total degree of polymerization (DP) of 409−481 and dispersity ($Đ$) of <1.16 (see Table 2). GPC analysis shows a uniform shift of the peaks to shorter elution time upon chain extension with HFANB (see Figure S6 in the Supporting Information), with no detectable terminated first block.

Vinyl addition random copolymers of HFANB and BuNB (a-RCP#, where # is the weight percentage of HFANB in the polymer) were synthesized via a slow dropwise addition of the monomer mixture into the reaction vessel (Scheme 1b). Adding the full charge of both monomers at the beginning, as is usual in batch copolymerizations, would lead to a strong BuNB-to-HFANB compositional gradient down the chain—resembling a diblock copolymer architecture—since BuNB adds much more rapidly than HFANB. However, with dropwise addition, since both monomers polymerize rapidly relative to the total time of monomer addition (~10 h), the monomer in each drop is essentially converted to polymer before the next drop is added, such that the polymer shows a negligible overall gradient in composition. Aliquots taken during the synthesis of a-RCP64 and quickly terminated, after approximately 1/3 and 2/3 of the monomer had been charged, revealed, via ^{1}H NMR spectroscopy, that the ratio of free to enchained monomer units was consistently <1%. The a-RCPs also show narrow and monomodal molecular weight distributions (see Figure S7 in the Supporting Information), with the exception of the most BuNB-rich copolymer (a-RCP37), which exhibited the same higher-M peaks noted above in BuNB homopolymerization (at $[BuNB]_0/[Pd]$ = 300) at long times. However, since these monomer-starved copolymerizations lead to negligible down-chain compositional gradients, a-RCP37 is still compositionally uniform, even if branched, so it was included in the pervaporation tests described below. SAXS (Figure S8 in the Supporting Information) and AFM (Figure S9 in the Supporting Information) reveal no evidence of microphase separation in the a-RCPs.

The vinyl addition block and random copolymers retain the high T_g and good thermal stability imparted by the saturated, bicyclic-ring backbone. No glass transition for any of the polymers was detected by differential scanning calorimetry (DSC) up to 200 °C;[28] the T_g values of polyBuNB and polyHFANB have been previously reported as 340 and 360 °C, respectively,[29] but polymer decomposition at such high temperatures makes an accurate determination of T_g difficult. Vinyl addition polyBuNB and polyHFANB exhibit insignificant weight loss until above 200 °C, with 5% weight loss occurring near 400 °C.[28]

The morphologies of the a-BCPs, cast from solution and solvent-annealed in THF, were characterized by SAXS and AFM. Figure 2 shows the SAXS patterns collected from relatively thick (~0.35 mm) films; all of the profiles contain a primary peak at a scattering vector magnitude $q = q^*$, which enables determination of the domain spacing ($d = 2\pi/q^*$). Higher-order peaks at $q = 2q^*$, $3q^*$, and $4q^*$ for a-BCP37, and at $q = \sqrt{3}q^*$ and $2q^*$ for a-BCP64, indicate morphologies of alternating polyBuNB and polyHFANB lamellae, and polyBuNB cylinders arranged on a hexagonal lattice in a polyHFANB matrix, respectively.

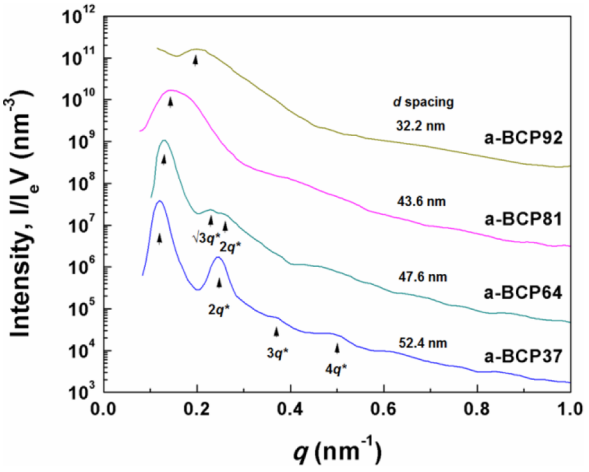

Figure 2. SAXS profiles of a-BCPs. Scattering intensity is plotted as a function of the magnitude of the scattering vector, q. Absolute intensities for patterns from polymers other than a-BCP37 are multiplied by successively larger factors to prevent overlap: $\times 10^2$ (a-BCP64), $\times 10^3$ (a-BCP81), and $\times 10^5$ (a-BCP92).

These same polymers were examined by AFM, in the form of the selective skin layers (~2 μm thick) on TFC membranes, whose cross section is schematized in Figure 3a. Uniform coating of the polymers on the supporting PAN-350 membrane was confirmed by SEM in both planar (Figure S10 in the Supporting Information) and cross-sectional views (see Figure 3b, as well as Figure S10 and Table S1 in the Supporting Information). Figure 3c shows the TM-AFM height images of the a-BCP selective layers; white and black domains are polyBuNB and polyHFANB, respectively. For these a-BCPs, AFM height images are more distinct than the corresponding phase images (Figure S11 in the Supporting Information), likely due to the similar stiffness of the high-T_g polyBuNB and polyHFANB domains. The images confirm the cylindrical morphology of a-BCP64, with a strong in-plane orientation of the polyBuNB cylinders; a-BCP92 and a-BCP81 show spherical morphologies with, at most, short-range order, consistent with the diffuse SAXS patterns observed for these polymers in Figure 2. A majority of the surface of a-BCP37 appears featureless, consistent with an in-plane arrangement of the lamellar domains evident by SAXS. Since a-BCP92, a-BCP81, and a-BCP64 all have continuous polyHFANB matrices, we do not anticipate a strong effect of domain orientation on pervaporation performance, although some influence might be expected for the lamella-forming a-BCP37.

The pervaporation performance of these membranes was evaluated using a home-built pervaporation apparatus (Scheme S2 in the Supporting Information), with 1.00 wt % n-BuOH aqueous feed, and measurements made at both 37 and 60 °C. Both flux and separation factor are higher at 60 °C; a temperature of 60 °C was employed for most measurements (see Figure S12 for pervaporation results for the a-BCP materials at 37 °C). The casting process led to somewhat different selective layer thicknesses across the different membranes (1.2−2.5 μm; see Table S1), because of differences in casting solution viscosity; to account for this variation, the flux was normalized (J') to an average membrane thickness of 2 μm. Figure 4a presents the data for the a-BCP membranes, while Figure 4b presents the data for the a-RCP membranes. Both block and random copolymers show a continuous and rapid (faster-than-linear) reduction in J' as W_{HFANB} is reduced,

DOI: 10.1021/acs.chemmater.5b03030
Chem. Mater. 2015, 27, 6791−6801

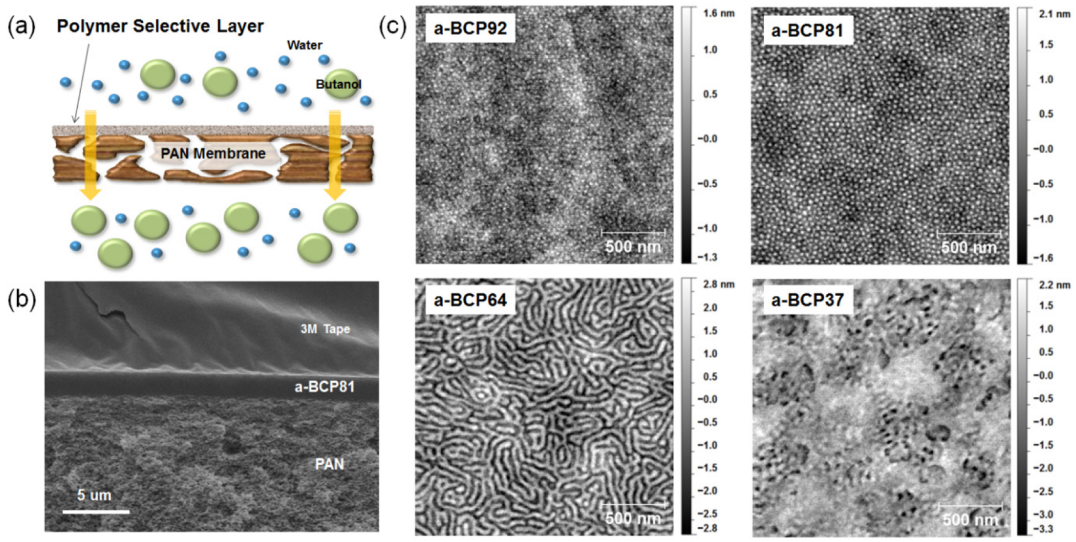

Figure 3. (a) Schematic illustration of membrane structure for butanol pervaporation recovery. (b) Cross-sectional SEM image of a-BCP81 membrane. (c) AFM height images of four a-BCP membrane surfaces (a-BCP92 (top left), a-BCP81 (top right), a-BCP64 (bottom left), and a-BCP37 (bottom right)).

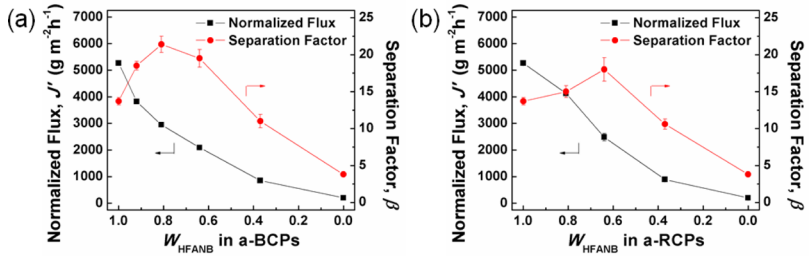

Figure 4. Effect of W_{HFANB} on pervaporation performance of (a) a-BCP and (b) a-RCP membranes for a 1.00 wt % *n*-BuOH feed at 60 °C: normalized flux $J' = J \times l/l_0$ ($l_0 = 2$ μm). Error bars reflect ±1 standard deviation in both J' and β from replicate measurements; for J', error bars are smaller than the symbols. Symbols at $W_{HFANB} = 1$ and 0 correspond to polyHFANB and polyBuNB homopolymers, respectively.

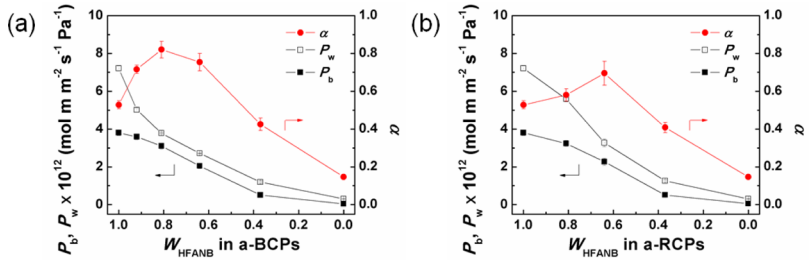

Figure 5. Effect of W_{HFANB} on intrinsic pervaporation performance of (a) a-BCP and (b) a-RCP membranes for a 1.00 wt % *n*-BuOH feed at 60 °C: permeabilities P_b (*n*-BuOH) and P_w (water), and membrane selectivity α. Error bars are based on replicate measurements of J' and β and do not include any contribution from the uncertainty in thermodynamic parameters (notably γ_b), which would scale all points equally. Symbols at W_{HFANB} = 1 and 0 correspond to polyHFANB and polyBuNB homopolymers, respectively.

and both show a maximum in the separation factor β at an intermediate value of W_{HFANB}, although the value of W_{HFANB} at the maximum differs slightly between the two cases.

While β and J' represent the practical quantities associated with the pervaporation operation (the quality and rate of the separation between the two components), they include contributions not only from the membrane but also from the component and solution thermodynamics (saturation vapor pressures and liquid-phase activity coefficients). To isolate the contribution made by the membrane, the permeabilities of water (P_w) and *n*-BuOH (P_b), along with the membrane selectivity α, were calculated as described in the Experimental Section; these quantities are plotted in Figure 5a for the a-BCP membranes, and in Figure 5b for the a-RCP membranes. As expected, the permeabilities of both components decrease as W_{HFANB} is reduced (W_{BuNB} is increased), although P_w decreases more rapidly than P_b at low W_{BuNB} in both block and random copolymers. The plots of membrane selectivity α (Figure 5) have the same shape as those for the process separation factor β (Figure 4), as the two quantities are simply related by a proportionality constant (dependent on feed composition and temperature; for a 1.00 wt % *n*-BuOH feed at 60 °C, $\alpha = \beta/25.9$). Note that the maximum value of α is 0.82 (for a-BCP81), indicating that the best of these membranes is essentially

DOI: 10.1021/acs.chemmater.5b03030
Chem. Mater. 2015, 27, 6791−6801

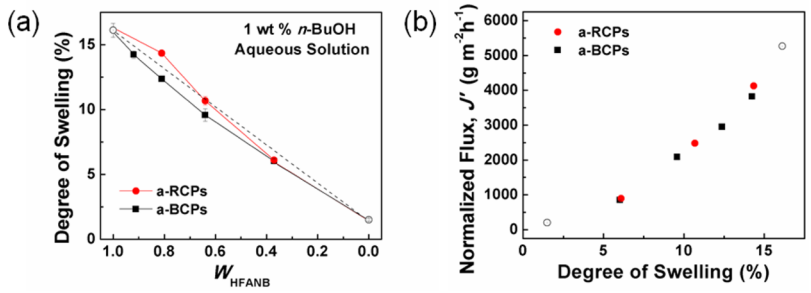

Figure 6. (a) Degree of swelling (DS) of a-BCP and a-RCP thick films (thickness of ~50 μm) with different W_{HFANB} in 1.00 wt % aqueous *n*-BuOH at room temperature. Open symbols at W_{HFANB} = 1 and 0 correspond to polyHFANB and polyBuNB homopolymers, respectively; dashed line connecting the two represents the weighted average. (b) Normalized flux (J') vs degree of swelling (DS) for a-BCPs and a-RCPs. Open symbols correspond to polyBuNB (lowest DS) and polyHFANB (highest DS) homopolymers.

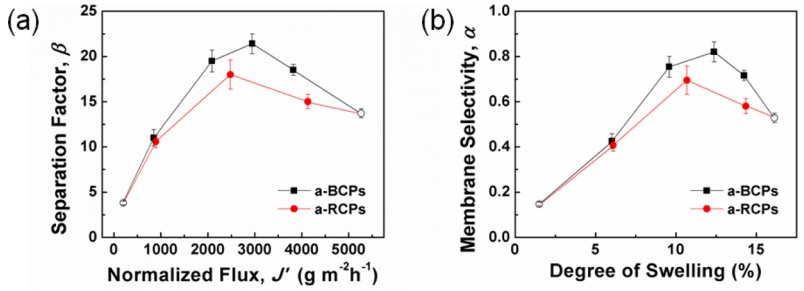

Figure 7. (a) Separation factor (β) vs thickness-normalized flux (J') for addition-polymer membranes formed from block copolymers (a-BCPs, black squares) and random copolymers (a-RCPs, red circles). Open symbols correspond to polyHFANB (highest J') and polyBuNB (lowest J') homopolymers. (b) Membrane selectivity (α) vs degree of swelling (DS), showing the same trends as panel a.

nonselective for the transport of *n*-BuOH over water; the substantial process separation factors evident in Figure 4 result principally from the vapor–liquid equilibrium behavior of the butanol–water feed (specifically, the very high γ_b = 66, providing a strong thermodynamic driving force for butanol to leave the feed).

One might envision the following limiting case for transport through an ideally phase-separated block copolymer:[21,41] (a) transport occurs exclusively through one domain (here, the polyHFANB matrix), and (b) both permeating species are always dilute within the membrane, so dilute that the presence of one permeating species within the membrane has a negligible effect on the flux of the other species. In this case, the selectivity will always be equal to that of the transporting block (polyHFANB); increasing the fraction of BuNB domains simply decreases J' and P_i (by decreasing the fraction of material available for permeate transport, and increasing the tortuosity), without affecting β and α. However, the data of Figures 4a and 5a clearly show that incorporating the less-selective polyBuNB blocks into the copolymers actually increases the values of β and α, at least initially (up to W_{BuNB} = 1 − W_{HFANB} = 0.19). Since the flux of both water and *n*-BuOH through polyBuNB is quite low (see points corresponding to W_{HFANB} = 0 in both Figures 4 and 5), the initial increase in β and α with W_{BuNB} for the a-BCPs can result only from a violation of the second assumption: the permeating species (especially *n*-BuOH) are *not* dilute within the membrane, and swelling of the membrane (chiefly by *n*-BuOH) has a significant effect on the species flux. Since swelling is unlikely to affect the flux of both species identically, in this case, the selectivity can be strongly dependent on the composition of the matrix of the swollen block copolymer film (e.g., ratio of *n*-BuOH to HFANB units within the swollen polyHFANB matrix).

The swelling behavior of these materials thus provides further insight into their pervaporation performance. All of these polymers (including the polyHFANB and polyBuNB homopolymers) have a strong preference to absorb *n*-BuOH over water, as is evident from the *n*-BuOH absorption results in Table 2; however, polyHFANB homopolymer dissolves in neat *n*-BuOH, while polyBuNB does not. We therefore expect a monotonic decrease in the swelling as W_{HFANB} decreases. Figure 6a shows the degree of swelling (DS, expressed as an increase in weight percentage) of each of these polymers after equilibration against 1.0 wt % aqueous *n*-BuOH, where this qualitative expectation is borne out; however, there are clear differences between the a-BCP and a-RCP cases, where the incorporation of small amounts of BuNB in a block copolymer reduces the swell factor *more* than it reduces W_{HFANB}, while incorporation of the same low levels of BuNB in a random copolymer reduces the swell factor *less* than it reduces W_{HFANB} (compare with the dashed line in Figure 6a). These differences largely explain the differences in flux and permeability between the a-BCP and a-RCP cases evident in Figures 4 and 5; when J' is plotted against the swell factor (Figure 6b), the two datasets collapse together. Note that, with a 1.00 wt % *n*-BuOH feed and β < 22, the permeate is still mostly water (>80 wt %), so J' largely reflects the rate of water transport through the membrane; it is thus instructive to compare the behavior of the polyHFANB with pure water vs 1.00 wt % *n*-BuOH. In pure water, DS = 6.7%, and with a pure water feed, the normalized pervaporation flux (J') is equal to 3100 g m^{-2} h^{-1}; yet, in 1.00 wt % aqueous *n*-BuOH, DS = 16.1%, and the water (species) flux (J'_w) is equal to 4600 g m^{-2} h^{-1}. Clearly, the water flux through the membrane increases with DS (even when most of the swelling liquid is *n*-BuOH); swelling by *n*-BuOH accelerates the transport of both water and *n*-BuOH through the

DOI: 10.1021/acs.chemmater.5b03030
Chem. Mater. 2015, 27, 6791–6801

membrane. In particular, the higher swelling of a-RCP81 versus a-BCP81 (Figure 6a) is responsible for the higher flux through the former (Figure 4b) vs the latter (Figure 4a). However, it is also the source of the lower butanol selectivity for a-RCP81 versus a-BCP81.

Since all of the HFANB-rich polymers show good flux (J' > 1000 g m^{-2} h^{-1}), a more critical assessment of the membrane performance is provided by the process separation factor (β), or the membrane selectivity (here, $\alpha = \beta/25.9$). The data in Figures 4a and 4b are replotted as β vs J' in Figure 7a; the block copolymers consistently show a higher value of β for any value of J'. This behavior is mirrored in Figure 7b, where the block copolymers also show a higher membrane selectivity for any degree of swelling. In both the block and random cases, the interesting materials (high β, high J') are those with a majority content of HFANB; the low flux and selectivity of polyBuNB homopolymer severely limit the performance of BuNB-rich membranes, regardless of how the BuNB units are arranged.

The following picture thus emerges from the data in Figures 4−7. PolyHFANB homopolymer (α = 0.53) is poorly selective for *n*-BuOH transport, in part because of polyHFANB's extensive swelling, even when the feed concentration is only 1.00 wt % *n*-BuOH; this extensive swelling facilitates the transport of water as well as *n*-BuOH across the membrane. The swelling can be reduced by incorporating BuNB units, as polyBuNB scarcely swells; this reduced swelling slows the transport of water faster than it slows the transport of *n*-BuOH, leading to the initial increase in α with W_{BuNB}, which is evident in both Figures 5a (a-BCPs) and 5b (a-RCPs), and commensurate increases in β (Figure 4). However, polyBuNB is much less selective than polyHFANB, so how the BuNB units are distributed (block versus random) affects the overall selectivity, even at the same degree of swelling (Figure 7b). When the BuNB units are arranged in a block, they simply serve to limit the swelling of the polyHFANB matrix, by anchoring the HFANB blocks to glassy polyBuNB domains; note that all the block copolymers swell less than the linear combination of the two homopolymers (Figure 6a, compare with dashed line), indicating that the polyHFANB matrix in the block copolymers is less swollen than in polyHFANB homopolymer, thereby raising the value of α. Negligible transport occurs through the polyBuNB domains—both water and *n*-BuOH "diffuse around" them—so the relatively poor selectivity of polyBuNB does not adversely affect the selectivity of the membrane in the block copolymer case. On the other hand, when the swelling reduction is achieved by *random* copolymerization, more BuNB is needed (Figure 6a), and the BuNB units are intimately combined with the HFANB units, so that their poorer selectivity *does* impact the membrane's selectivity (see Figure 7b).

While the block copolymers consistently show a better balance of β and J' than the random copolymers (Figure 7a), it is worth noting that the random copolymers are not greatly inferior. Controlling the composition of the swollen HFANB-rich domains (i.e., the ratio of *n*-BuOH to HFANB units) evidently has a larger impact on the selectivity than the inclusion of some less-selective BuNB units in the transport pathway (in the a-RCP case). This suggests that control over the degree of swelling of polyHFANB might be achievable by other methods, such as cross-linking, at the expense of the simple membrane preparation method employed here.

The pervaporation performance of the ROMP-derived block copolymer, r-BCP81 (characteristics shown in Table 1, graphical synthetic outline presented in Scheme S1) provides further support to this interpretation. r-BCP81 is found to be microphase-separated by DSC (see Figure S13 in the Supporting Information; T_g = 39 °C for the hydrogenated polyHFANB domains, 0 °C for the hydrogenated polyBuNB domains), SAXS (Figure S14 in the Supporting Information), and AFM (Figure S15 in the Supporting Information), with a morphology of spheres of hydrogenated ROMP polyBuNB in a matrix of hydrogenated ROMP polyHFANB. However, while compositionally equivalent to a-BCP81, the ROMP polymer swells much more extensively in 1.0 wt % *n*-BuOH (DS = 32%), and the r-BCP81 membrane shows exceedingly high flux (J' = 12 000 g m^{-2} h^{-1}) but poor separation (β = 5.1, α = 0.20) for a 1.00 wt % *n*-BuOH feed at 60 °C, which is a much higher flux and lower *n*-BuOH selectivity than that obtained for the less-swollen a-BCP81 (Figure 4a).

It is instructive to compare our membranes against those with cross-linked poly(dimethylsiloxane) (PDMS) selective layers, because such PDMS membranes are already commercial products and have been extensively studied for organophilic pervaporation separations. Even for commercial PDMS-based membranes, the data are somewhat scattered, but for a 1.00 wt % *n*-BuOH feed, at 60 °C, values of β = 17−35 and fluxes J = 900−5000 g m^{-2} h^{-1} are estimated;[14,18] the membranes showing the highest J also exhibit the lowest β. Furthermore, a relatively thick (50 μm) PDMS membrane was reported[20] to show a process separation factor of β = 58 for 1.00 wt % aqueous *n*-BuOH at 50 °C (but a flux of only J = 70 g m^{-2} h^{-1}). The lower end of this β range ($\beta \approx$ 20−25) is similar to our results for a-BCP81 and a-RCP64, corresponding to a membrane selectivity of $\alpha \leq 1$; the upper end of this range (β = 58) corresponds to $\alpha \approx 2$. Some of the apparent variation in β across these PDMS-based membranes may reflect differences in cross-linking density or chemistry, while the variation in J surely also reflects differences in the selective layer thickness l.[18] From the data of Böddeker on relatively thick PDMS membranes,[20] a value of the *n*-butanol permeability of $P_b = 6.0 \times 10^{-12}$ mol m m^{-2} s^{-1} Pa^{-1} is calculated at 50 °C; this is roughly twice the values that we have measured for a-BCP81 and a-RCP64 at 60 °C (3.1×10^{-12} and 2.3×10^{-12} mol m m^{-2} s^{-1} Pa^{-1}, respectively).

While our a-BCP81 and a-RCP64 membranes exhibit comparable (but not superior) values of β, α, and P_b to commercial PDMS membranes, the vinyl addition polymers have a substantial practical advantage in flux (J), because of the ability to prepare very thin, but mechanically robust, selective layers from these high-T_g polymers. Figure 8 shows that a-BCP81 selective layers as thin as 1.3 μm were easily prepared, yielding fluxes as high as 4330 g m^{-2} h^{-1}; the separation factor is independent of selective layer thickness, indicating that even the thinnest membranes were substantially free from pinholes. We did not attempt to prepare selective layer thicknesses below 1.3 μm, so thinner layers may well be possible. Moreover, the simple hand-casting process we employed for membrane preparation could potentially be scaled up as a roll-to-roll slot-die or gravure coating process, without requiring the cross-linking reaction necessary for PDMS; the degree of control possible with such a continuous membrane fabrication process should allow even thinner selective layers to be prepared.

These robustness of these membranes was demonstrated by running the pervaporation process for an extended period (24 h; see Figure 9); no change in either J or β can be observed, indicating no loss of selective layer integrity. The microphase-

DOI: 10.1021/acs.chemmater.5b03030
Chem. Mater. 2015, 27, 6791−6801

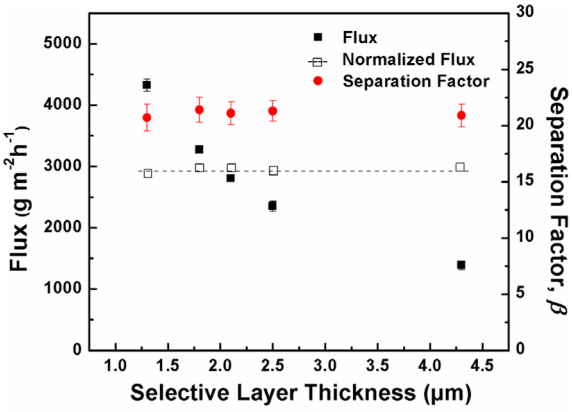

Figure 8. Effect of thickness on pervaporation performance of a-BCP81 membranes for a 1.00 wt % *n*-BuOH aqueous feed at 60 °C. Normalized flux $J' = J \times l/l_0$ ($l_0 = 2$ μm). The selective layer thickness l was controlled through the concentration of the coating solution and the gap height of the film casting knife.

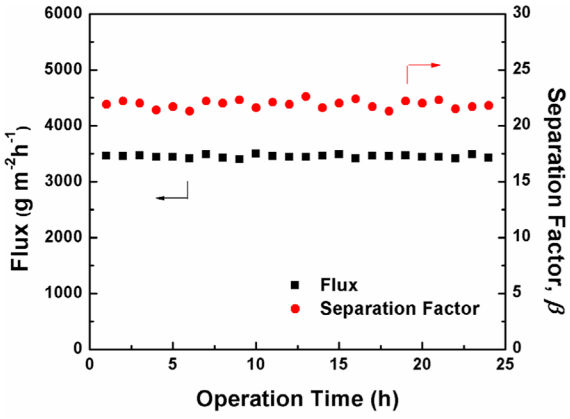

Figure 9. Stability of pervaporation performance of a-BCP81 membrane (1.7 ± 0.1 μm selective layer thickness) with a 1.00 wt % *n*-BuOH aqueous feed at 60 °C.

separated morphology of the a-BCP81 selective layer was unchanged after 24 h of pervaporation (Figure S16 in the Supporting Information).

CONCLUSIONS

We have used a new living polymerization initiator complex to synthesize two series of well-defined vinyl addition copolymers of HFANB and BuNB, with either block or random sequence, and we have investigated these polymers as membranes for the recovery of *n*-BuOH from dilute aqueous solution. Although the polymers are substantially swollen when in contact with 1.00 wt % aqueous *n*-BuOH, they remain glassy in the swollen state, because of the high glass-transition temperature (T_g) of the neat polymers. Both block and random vinyl addition copolymers are effective as pervaporation membranes, with *n*-BuOH process separation factors $\beta > 10$ (as high as $\beta = 21.4$); the incorporation of modest levels of BuNB into polyHFANB (<40 wt %) reduces the swelling of polyHFANB, thereby reducing the flux and improving the selectivity. While the thickness-normalized flux J' through any of these addition polymers (block or random) was essentially determined solely by its level of swelling, the membrane selectivity α of the block copolymers at a given degree of swelling was higher than that of the random copolymers, since the relatively nonselective BuNB units are not in the transport pathway in the microphase-separated block copolymers. The importance of limited swelling for pervaporation performance was highlighted by comparison with an analogous ROMP-derived block copolymer, which showed much higher swelling, higher flux, and lower selectivity. We believe that the present work provides insight into the design of high-T_g block copolymers of substituted NB monomers for application as membranes, both for pervaporation as well as other types of separations, by taking advantage of the diversity of available substituent groups[28] to tune permeability and selectivity.

ASSOCIATED CONTENT

Supporting Information

The Supporting Information is available free of charge on the ACS Publications website at DOI: 10.1021/acs.chemmater.5b03030.

Graphical schemes of ROMP synthesis and pervaporation apparatus; GPC and NMR data of vinyl addition homopolymers and copolymers; SAXS profiles and AFM images of a-RCPs; SEM and AFM characterization of membranes; pervaporation performance of a-BCP membranes at 37 °C; DSC, SAXS, and AFM characterization of r-BCP81 (PDF)

AUTHOR INFORMATION

Corresponding Author

*E-mail: register@princeton.edu.

Notes

The authors declare no competing financial interest.

ACKNOWLEDGMENTS

This work was supported by Promerus, LLC and the Princeton University Innovation Fund for Industrial Collaboration. The authors gratefully acknowledge Douglas Greer and Nitash Balsara (University of California, Berkeley) for helpful discussions regarding thermodynamic data for the *n*-butanol–water mixtures.

REFERENCES

(1) Grove, N. R.; Kohl, P. A.; Bidstrup Allen, S. A.; Jayaraman, S.; Shick, R. Functionalized Polynorbornene Dielectric Polymers: Adhesion and Mechanical Properties. *J. Polym. Sci., Part B: Polym. Phys.* **1999**, *37*, 3003–3010.

(2) Blank, F.; Janiak, C. Metal Catalysts for the Vinyl/Addition Polymerization of Norbornene. *Coord. Chem. Rev.* **2009**, *253*, 827–861.

(3) Oh, S.; Lee, J.-K.; Theato, P.; Char, K. Nanoporous Thin Films Based on Polylactide-Grafted Norbornene Copolymers. *Chem. Mater.* **2008**, *20*, 6974–6984.

(4) Okoroanyanwu, U.; Shimokawa, T.; Byers, J.; Willson, C. G. Alicyclic Polymers for 193 nm Resist Applications: Synthesis and Characterization. *Chem. Mater.* **1998**, *10*, 3319–3327.

(5) Tran, H. V.; Hung, R. J.; Chiba, T.; Yamada, S.; Mrozek, T.; Hsieh, Y.-T.; Chambers, C. R.; Osborn, B. P.; Trinque, B. C.; Pinnow, M. J.; MacDonald, S. A.; Willson, C. G.; Sanders, D. P.; Connor, E. F.; Grubbs, R. H.; Conley, W. Metal-Catalyzed Vinyl Addition Polymers for 157 nm Resist Applications. 2. Fluorinated Norbornenes: Synthesis, Polymerization, and Initial Imaging Results. *Macromolecules* **2002**, *35*, 6539–6549.

(6) Park, K. H.; Twieg, R. J.; Ravikiran, R.; Rhodes, L. F.; Shick, R. A.; Yankelevich, D.; Knoesen, A. Synthesis and Nonlinear-Optical

DOI: 10.1021/acs.chemmater.5b03030
Chem. Mater. 2015, 27, 6791–6801

Properties of Vinyl-Addition Poly(norbornene)s. *Macromolecules* **2004**, *37*, 5163−5178.
(7) Finkelshtein, E. S.; Makovetskii, K. L.; Gringolts, M. L.; Rogan, Y. V.; Golenko, T. G.; Starannikova, L. E.; Yampolskii, Y. P.; Shantarovich, V. P.; Suzuki, T. Addition-Type Polynorbornenes with $Si(CH_3)_3$ Side Groups: Synthesis, Gas Permeability, and Free Volume. *Macromolecules* **2006**, *39*, 7022−7029.
(8) Chen, L.; Wang, X.; He, X.; Liu, S.; Chen, Y.; Zhou, W. Vinyl-addition Type Norbornene Copolymer Containing Sulfonated Biphenyl Pendant Groups for Proton Exchange Membranes. *J. Appl. Polym. Sci.* **2013**, *127*, 2280−2289.
(9) Lin, Y.; Tanaka, S. Ethanol Fermentation from Biomass Resources: Current State and Prospects. *Appl. Microbiol. Biotechnol.* **2006**, *69*, 627−642.
(10) Qureshi, N.; Ezeji, T. C. Butanol, "a Superior Biofuel" Production From Agricultural Residues (Renewable Biomass): Recent Progress in Technology. *Biofuels, Bioprod. Biorefin.* **2008**, *2*, 319−330.
(11) Abdehagh, N.; Tezel, F. H.; Thibault, J. Separation Techniques in Butanol Production: Challenges and Developments. *Biomass Bioenergy* **2014**, *60*, 222−246.
(12) Liu, G.; Wei, W.; Jin, W. Pervaporation Membranes for Biobutanol Production. *ACS Sustainable Chem. Eng.* **2014**, *2*, 546−560.
(13) Shao, P.; Huang, R. Y. M. Polymeric Membrane Pervaporation. *J. Membr. Sci.* **2007**, *287*, 162−179.
(14) Jonquières, A.; Fane, A. Filled and Unfilled Composite GFT PDMS Membranes for the Recovery of Butanols from Dilute Aqueous Solutions: Influence of Alcohol Polarity. *J. Membr. Sci.* **1997**, *125*, 245−255.
(15) Claes, S.; Vandezande, P.; Mullens, S.; De Sitter, K.; Peeters, R.; Van Bael, M. K. Preparation and Benchmarking of Thin Film Supported PTMSP-Silica Pervaporation Membranes. *J. Membr. Sci.* **2012**, *389*, 265−271.
(16) Li, S.; Qin, F.; Qin, P.; Karim, M. N.; Tan, T. Preparation of PDMS Membrane Using Water as Solvent for Pervaporation Separation of Butanol-Water Mixture. *Green Chem.* **2013**, *15*, 2180−2190.
(17) Niemistö, J.; Kujawski, W.; Keiski, R. L. Pervaporation Performance of Composite Poly(dimethyl siloxane) Membrane for Butanol Recovery from Model Solutions. *J. Membr. Sci.* **2013**, *434*, 55−64.
(18) Rozicka, A.; Niemistö, J.; Keiski, R. L.; Kujawski, W. Apparent and Intrinsic Properties of Commercial PDMS Based Membranes in Pervaporative Removal of Acetone, Butanol and Ethanol from Binary Aqueous Mixtures. *J. Membr. Sci.* **2014**, *453*, 108−118.
(19) Shin, C.; Baer, Z. C.; Chen, X. C.; Ozcam, A. E.; Clark, D. S.; Balsara, N. P. Block Copolymer Pervaporation Membrane for *In Situ* Product Removal During Acetone−Butanol−Ethanol Fermentation. *J. Membr. Sci.* **2015**, *484*, 57−63.
(20) Böddeker, K. W.; Bengtson, G.; Pingel, H. Pervaporation of Isomeric Butanols. *J. Membr. Sci.* **1990**, *54*, 1−12.
(21) Greer, D. R.; Ozcam, A. E.; Balsara, N. P. Pervaporation of Organic Compounds from Aqueous Mixtures Using Polydimethylsiloxane-Containing Block Copolymer Membranes. *AIChE J.* **2015**, *61*, 2789−2794.
(22) Liu, S.; Liu, G.; Shen, J.; Jin, W. Fabrication of MOFs/PEBA Mixed Matrix Membranes and Their Application in Bio-butanol Production. *Sep. Purif. Technol.* **2014**, *133*, 40−47.
(23) Fadeev, A. G.; Selinskaya, Y. A.; Kelley, S. S.; Meagher, M. M.; Litvinova, E. G.; Khotimsky, V. S.; Volkov, V. V. Extraction of Butanol from Aqueous Solutions by Pervaporation Through Poly(1-trimethylsilyl-1-propyne). *J. Membr. Sci.* **2001**, *186*, 205−217.
(24) Wijmans, J. G.; Baker, R. W. The Solution-Diffusion Model—A Review. *J. Membr. Sci.* **1995**, *107*, 1−21.
(25) Knapp, B.; Elce, E.; Bedwell, B.; Langsdorf, L. J.; Wilks, R. J. C. (Promerus LLC). Polynorbornene Pervaporation Membrane Films, Preparation and Use Thereof. U.S. Patent 8,215,496, July 10, 2012.
(26) Bielawski, C. W.; Grubbs, R. H. Living Ring-Opening Metathesis Polymerization. *Prog. Polym. Sci.* **2007**, *32*, 1−29.
(27) Yamashita, M.; Takamiya, I.; Jin, K.; Nozaki, K. Syntheses and Structures of Bulky Monophosphine-ligated Methylpalladium Complexes: Application to Homo- and Copolymerization of Norbornene and/or Methoxycarbonylnorbornene. *Organometallics* **2006**, *25*, 4588−4595.
(28) Kim, D.-G.; Bell, A.; Register, R. A. Living Vinyl Addition Polymerization of Substituted Norbornenes by a *t*-Bu_3P-Ligated Methylpalladium Complex. *ACS Macro Lett.* **2015**, *4*, 327−330.
(29) Ye, C.; Takigawa, T.; Burtovvy, O.; Langsdorf, L.; Jablonski, D.; Bell, A.; Vogt, B. D. Impact of Nanostructure on Mechanical Properties of Norbornene-based Block Copolymers under Simulated Operating Conditions for Biobutanol Membranes. *ACS Appl. Mater. Interfaces* **2015**, *7*, 11765−11774.
(30) Lee, E. J.; Won, W. K.; Lee, B.; Kye, Y. H.; Lee, I. M. Novel Pd Catalysts with β-Diketiminates for Homopolymerization of Functionalized Norbornene Derivatives in Water/Organic Mixed Solvents. *Bull. Korean Chem. Soc.* **2013**, *34*, 2720−2724.
(31) Bell, A.; Rhodes, L. F.; Goodall, B. L.; Fondran, J. C. (B.F. Goodrich Company). Mold Addition Polymerization of Norbornene-type Monomers Using Group 10 Metal Complexes. U.S. Patent 6,350,832, Feb. 26, 2002.
(32) Lipian, J.; Mimna, R. A.; Fondran, J. C.; Yandulov, D.; Shick, R. A.; Goodall, B. L.; Rhodes, L. F.; Huffman, J. C. Addition Polymerization of Norbornene-type Monomers. High Activity Cationic Allyl Palladium Catalysts. *Macromolecules* **2002**, *35*, 8969−8977.
(33) Baker, R. W.; Wijmans, J. G.; Huang, Y. Permeability, Permeance and Selectivity: A Preferred Way of Reporting Pervaporation Performance Data. *J. Membr. Sci.* **2010**, *348*, 346−352.
(34) Fischer, K.; Gmehling, J. *P-x* and γ^{∞} Data for the Different Binary Butanol−Water Systems at 50 °C. *J. Chem. Eng. Data* **1994**, *39*, 309−315.
(35) Gmehling, J.; Onken, U. *Vapor−Liquid Equilibrium Data Collection*, Vol. *1*, Part 1; DECHEMA: Frankfurt, Germany, 1977; p 411.
(36) Schreiber, E.; Schüettau, E.; Rant, D.; Schuberth, H. Die Beeinflußbarkeit des Isothermen Phasengleichgewichtsverhaltens der Systeme *n*-Propanol/Wasser und *n*-Butanol/Wasser durch Einige Metallchloride. *Z. Phys. Chem. (Leipzig)* **1971**, *247*, 23−40.
(37) Hatjopoulos, J. D.; Register, R. A. Synthesis and Properties of Well-Defined Elastomeric Poly(alkylnorbornene)s and Their Hydrogenated Derivatives. *Macromolecules* **2005**, *38*, 10320−10322.
(38) Bushuk, W.; Benoît, H. Light-Scattering Studies of Copolymers. 1. Effect of Heterogeneity of Chain Composition on the Molecular Weight. *Can. J. Chem.* **1958**, *36*, 1616−1626.
(39) Register, R. A.; Bell, T. R. Miscible Blends of Zinc-Neutralized Sulfonated Polystyrene and Poly(2,6-dimethyl 1,4-phenylene oxide). *J. Polym. Sci., Part B: Polym. Phys.* **1992**, *30*, 569−575.
(40) Huang, T. C.; Toraya, H.; Blanton, T. N.; Wu, Y. X-ray Powder Diffraction Analysis of Silver Behenate, a Possible Low-Angle Diffraction Standard. *J. Appl. Crystallogr.* **1993**, *26*, 180−184.
(41) Ozcam, A. E.; Petzetakis, N.; Silverman, S.; Jha, A. K.; Balsara, N. P. Relationship between Segregation Strength and Permeability of Ethanol/Water Mixtures through Block Copolymer Membranes. *Macromolecules* **2013**, *46*, 9652−9658.

DOI: 10.1021/acs.chemmater.5b03030
Chem. Mater. 2015, 27, 6791−6801